

Comparative Binding and Uptake of liposomes decorated with mannose oligosaccharides by cells expressing the mannose receptor or DC-SIGN

Haifei Gao¹, Cristine Gonçalves¹, Téo Gallego², Marc François-Heude², Virginie Malard¹,
Véronique Mateo³, François Lemoine³, Virginie Cendret², Florence Djedaini-Pilard², Vincent
Moreau² and Chantal Pichon^{1*} and Patrick Midoux^{1*}

¹Centre de Biophysique Moléculaire, CNRS UPR4301, Inserm and University of Orléans, F-45071, Orléans cedex 02, France.

²Laboratoire de Glycochimie, des Antimicrobiens et des Agroressources, LG2A UMR7378, ICP FR 3085, Université de Picardie Jules Verne, 80039 Amiens Cedex.

³Sorbonne University, UMR-S INSERM U1135, CNRS ERL 8255, Centre d'Immunologie et Maladies Infectieuses (CIMI-Paris), Paris, France.

*to whom correspondence should be addressed: Patrick.midoux@cnrs-orleans.fr;

Chantal.pichon@cnrs.fr

ORCID

Florence Djedaini-Pilard: 0000-0002-2841-0023

Patrick Midoux: 0000-0002-8762-366X

Key words: oligosaccharides; glycolipids; liposomes; dendritic cells; Mannose Receptor; DC-SIGN

Abstract

Mannose Receptor (MR) and DC-specific intercellular adhesion molecule-3-grabbing non-integrin (DC-SIGN) are two mannose-specific targets for antigens carried by liposomes but DC-SIGN is more specific of DCs. Here, DC targeting is addressed by using DPPC/DOPE liposomes decorated with a series of diether lipids with a polar head of either a mannose (Man), tri-antenna of α -D-mannopyranoside (Tri-Man), [Man α 1-3(Man α 1-6)Man] (Man-tri), pseudo-Man₄ (PMan₄) or pseudo-Man₅ (PMan₅). Liposomes decorated with Man-Tri show the highest binding and internalization in cells expressing DC-SIGN and in human monocytes-derived DCs. Conversely, cells expressing MR bind and take up Tri-Man liposomes 3-fold higher than Man-tri liposomes. Comparatively, liposomes decorated with PMan₄ and PMan₅ do not show any advantages. Overall, the results indicate that liposomes decorated with Man-tri residues are more selective toward DCs than those with Tri-Man thanks to better recognition by DC-SIGN.

1. Introduction

Dendritic cells (DCs) are the most powerful professional antigen presenting cells for cancer immunotherapy by inducing cytotoxic CD8⁺ T lymphocytes against tumor cells [1-4]. Nowadays, antigens can be proteins, peptides, DNA or mRNA [5-12]. However, a selective transport of antigens is required to favor their intracellular delivery in DCs *in vivo*. For this purpose, liposomes are powerful carriers and their decoration with ligands recognizing specific receptors on DC surface can improve the targeting and endocytosis of antigens. Carbohydrate-based targeting is an obvious manner to enhance the capture and uptake by DCs of antigen pay loaded liposomes because DCs express several sugar receptors binding oligosaccharides [13-16]. The Mannose Receptor (MR) (CD206) and the DC-specific intercellular adhesion molecule-3-grabbing non-integrin (DC-SIGN) (CD209) induce a clathrin-dependent mediated endocytosis of terminal “high-mannose oligosaccharides”. In contrast to MR expressed also in various kind of cells including monocytes, macrophages, subsets of endothelial cells, retinal pigment epithelium, kidney mesangial cells, and tracheal smooth muscle cells, DC-SIGN is only expressed by DCs [17]. In humans, DCs in mucosal sites, skin and lymph nodes express preponderantly DC-SIGN [18]. It is not expressed by monocytes, activated monocytes, T cells, activated T cells, B cells, activated B cells and CD34⁺ bone marrow cells. DC-SIGN expressing cells are present in the T cell area of lymph nodes, tonsils and spleens. In skin, dermal DCs express DC-SIGN but not Langerhans cells

nor macrophages. Mature DCs only express DC-SIGN allowing the endocytosis of antigens and their presentation by the MHC type I and II [18-21]. In blood, plasmacytoid DCs do not express DC-SIGN while myeloid DCs do. DC-SIGN plays an important role in DCs adhesion to naive T lymphocytes and endothelium of blood and lymphatic vessels, in their migration, in inflammation, in the activation of primary T cells, and in triggering of the immune response [22]. While MR recognizes mannose located at the end of the carbohydrate chains, DC-SIGN preferentially binds to branched mannose [16]. DC-SIGN recognizes also fucosylated glycans such as the blood-type Lewis antigens (Le^a , Le^b , Le^x , Le^y , and sulfo- Le^a) [23]. Liposomes decorated with Lewis antigens were used to deliver tumor antigens and induce anti-tumour T cell responses [24, 25]. Thus, targeting this receptor would both increase uptake and reduce the antigen dilution after *in vivo* administration. α -D-mannopyranosyl derivatives are usually used because they are available under forms that can be easily conjugated to various carriers but the binding affinity typically is weak ($K \sim 10^{-3} \text{ M} - 10^{-4} \text{ M}$). The multivalent decoration of proteins, polymers or liposomes with monosaccharide units increases the apparent affinity by 1 or 2 orders of magnitude [26, 27]. High-mannose oligosaccharides such as Man_9 and Man_8 exhibiting high affinity ($K = 10^{-6} \text{ M}$) for membrane lectins should be more attractive targeting ligands, but their synthesis is hard, expensive and yields are weak. Therefore, pseudo- Man_9 (P Man_9), pseudo- Man_8 (P Man_8), pseudo- Man_5 (P Man_5) and pseudo- Man_4 (P Man_4) mimicking the High-mannose oligosaccharides or moieties were synthesized in which triazole groups

replaced some mannopyranosyl residues [28, 29]. PMan₄ mimics the Man α 1-2Man α 1-2Man α 1-3Man tetrasaccharide (D1 arm) of Man₉; PMan₅ the Man α 1-2Man α 1-6 (Man α 1-2Man α 1-3)Man α 1- pentasaccharide (D2 and D3 arms) of Man₉ and Man₈; Man-tri the Man α 1-6(Man α 1-3)Man α 1- trisaccharide (D2 and D3 arms) of Man₅, Man₆ and Man₇ (Supplementary Figure 1). Interestingly, affinities of the same order of magnitude against lectins were observed for pseudo-Man_n/Man_n pairs in the case of the higher homologues supporting their functional equivalency. The relative affinity of PMan₉, PMan₈ and PMan₅ was ~2-fold lower than Man₉, Man₈ and Man₅, respectively [29]. Compared to the methy- α -D-mannoside (Me α Man) the relative affinity of PMan₅, PMan₄ and Man-tri with Concanavalin A (ConA) was 20.8-, 3.8-, and 11-fold higher, respectively and with the recombinant human macrophage mannose receptor it was 30.6-, 2.12- and 10-fold higher, respectively [29].

In this work, we synthesized a series of glycolipids comprising either mannose, a tri-antenna of α -D-mannopyranoside, the [Man α 1-3(Man α 1-6)Man], the pseudo-Man₄ or the pseudo-Man₅. Next, we compared the binding and uptake of a series of fluorescein-labelled liposomes decorated with these glycolipids by DC2.4 cells expressing the mannose receptor, DC-SIGN HEK293T cells expressing DC-SIGN and human monocytes derived DCs (hMo-DCs).

2. Results and discussion

2.1. Synthesis of Mannosylated lipids and liposomes preparation

A series of new glycolipids (**2-7**) similar to the Tri-Man diether lipid **1** (Figure 1A) was synthesized comprising an archaeal diether lipid linked *via* an oligoethylene spacer to one of the mannose structures (Figure 1B) [30]. Archaeal lipids exhibiting adjuvant properties independent on Toll-like receptors activation could be benefit to boost the immune response [31-33]. Thus, various azido glycosides (**2a-7a**) were linked by “click chemistry” to the diether lipid with more than 95% of yield leading to glyco-diether lipids **2-7**. For this purpose, the propargyl-PEG₈-diether was synthesized (Figure 2).

Then, fluorescein-labelled liposomes (Flu-Lip) were prepared comprising DPPC (47.25%), DOPE (47.25%), one glyco-diether lipid (5%) and Flu-DOPE (0.5%) (Supplementary Figure 2). The corresponding liposomes (**1b-7b**) exhibited a size of ~150 nm in diameter and a negative ζ potential varying with the sugar polar head nature (Table I).

2.2. Binding to mannose specific lectins

The binding of the liposomes to ConA and BC2LA was evaluated as a function of their oligomannose structures. The Flu-Lip equipped with Tri-Man (**1**), Man-tri (**4**), PMan₄ (**6**) and PMan₅ (**7**) showed better and similar apparent binding to ConA than with Man (**3**) (Figure 3A).

The binding profile was similar with BC2LA excepted that the binding of Man-tri-spa (**5b**) was lower than Man-tri (**4b**) (Figure 3B). There was a weak binding of Glc (**2b**) due to a small affinity of ConA for α -D-glucosyl residues. In contrast, Glc (**2b**) did not interact with BC2LA. Thus, those oligomannose structures conserved their binding capacity to lectins after their linkage to the diether lipid and insertion in the lipid bilayer of liposomes. The results were in agreement with data reported in literature indicating that compared to Me α Man, the relative affinity to ConA of a tri-antenna mannopyranoside, PMan₅ (**7a**), PMan₄ (**6a**) and Man-tri (**4a**) was 16-, 20.8-, 3.8- and 11-fold, respectively [29]. Here, the binding of liposomes PMan₄ (**6b**) was similar to PMan₅ (**7b**).

2.3. Binding and uptake of liposomes by DC2.4 cells and DC-SIGN expressing HEK293 cells

DC2.4 cells express the MR while DC-SIGN HEK293 cells express only DC-SIGN (Supplementary Figure 3). Flow cytometry was used to assess the binding and uptake of Flu-Lip by these cells and analyses were performed as described in Supplementary Figure 4. The mean of the fluorescence intensity (MFI) of cells incubated with Flu-Lip was first measured without any treatment (NT), the second time in the presence of Trypan blue (TB) and the third time in the presence of monensin (MO). The MFI decrease upon TB treatment quenching fluorescein fluorescence on the cell surface indicated that ~ 70% of liposomes associated to the cells were bound on the cell surface; the remaining MFI came from the fluorescence of intracellular liposomes. The MFI increase upon MO treatment raising the quenching of the

fluorescein fluorescence in acid intracellular compartments indicated that liposomes trafficked through endosomes and lysosomes.

This series of MFI measurements allowed determination of the amount of liposomes bound and internalized by the cells and thanks to the MO treatment the type of uptake. On this base, the cell surface binding upon 3h incubation at 37°C was determined from MFI measured without any treatment minus MFI measured in the presence of TB. Of note: cells were harvested without trypsin in order to prevent harvesting of liposomes bound on the cell surface.

The intracellular quantity of liposomes was determined from MFI measured upon monensin treatment - which rose the fluorescein fluorescence quenched in acid intracellular compartments such as endosomes and lysosomes - minus fluorescence ($MFI - MFI_{TB}$) corresponding to liposomes bound on the cell surface. Moreover, increased MFI upon monensin treatment meant that liposomes uptake likely occurred through acidic compartments such as endosomes and lysosomes, presumably *via* clathrin-dependent endocytosis. Although, Tri-Man (**1b**) bound more on the surface of DC2.4 cells, their intracellular quantity was close to that observed with Man (**3b**), Man-tri-spa (**5b**) and PMan₄ (**6b**) (Figure 4Ba).

In cells expressing DC-SIGN, the highest binding and internalization was observed with Man-tri (**4b**). The uptake was 2- to 3-fold higher than with Tri-Man (**1b**), PMan₄ (**6b**) and PMan₅ (**7b**) (Figure 4Bb). The monensin enhancement was lower (< 2.5) in DC2.4 cells (Figure 4Ca)

than in DC-SIGN HEK293 cells (> 4) (Figure 4Cb). In the latter cells, this enhancement increased with liposomes concentration indicating that liposomes accumulated in acidic compartments. In DC2.4 cells, the monensin enhancement for Man-tri (**4b**) and Man-tri-spa (**5b**) (even Tri-Man (**1b**)) was high at low concentration and then dropped to even the value of 1 meaning that fluorescein was in a neutral environment which could result from escape of liposomes from acidic compartments. However, it was difficult to conclude about different intracellular processing of liposomes internalized *via* MR or DC-SIGN because the cell types were different. Altogether, the results indicated that Man-tri (**4b**) provided better uptake by DC-SIGN positive cells than MR positive cells. Conversely, we observed better selectivity and uptake of Tri-Man (**1b**) by MR positive cells. MR is a monomeric membrane-bound protein allowing mannose binding to two (or more) separate but interacting carbohydrate recognition domains (CRDs) within the mannose receptor [34-36]. The structure of the tri-antenna α -mannopyranoside in Tri-Man (**1**) is more adapted to bind to separate CRDs of MR than the tri-mannose structure of Man-tri (**4**). Conversely, the presence of the branching $\alpha(1,2)$ mannose on Man-Tri (**4b**) increases their binding toward DC-SIGN as reported [37]. Comparatively, PMan₄ (**6**) and PMan₅ (**7**) did not provide benefit in terms of binding and uptake of the liposomes.

2.4. Binding and uptake of liposomes by hMo-DCs

The same experiments were performed on hMo-DCs that expressed both MR and DC-SIGN. The MFI on the surface of the cells incubated with Tri-Man (**1b**), Man-tri (**4b**), Man-tri-spa (**5b**), PMan₄ (**6b**), and PMan₅ (**7b**) was saturable indicating a receptor mediated binding of those liposomes (Figure 5A).

In contrast, the binding of Man (**3b**) increased linearly with the concentration and was not saturable. The intracellular MFI of Man-tri-spa (**5b**) was higher than Man-tri (**4b**) and it was much higher than Tri-Man (**1b**) (Figure 5B). The intracellular MFI with PMan₄ (**6b**) was close to that with Tri-Man (**1b**) but higher than with PMan₅ (**7b**).

3. Conclusion

This work revealed that decorating DPPC/DOPE liposomes with a tri-antenna α -mannopyranoside (Tri-Man) (**1**) is beneficial for targeting liposomes to MR while decoration with a [Man α 1-3(Man α 1-6)Man] (Man-tri) (**4**) is beneficial for targeting DC-SIGN. Compared to Tri-Man (**1**) and Man-tri (**4**), there was no great benefit to use other complex mannose structures such as PMan₄ (**6**) and PMan₅ (**7**) in terms of binding and uptake efficiency. In contrast to MR expressed in various kind of cells, DC-SIGN is expressed preponderantly on DCs at mucosal sites, in skin and lymph nodes in humans. In skin, DCs express DC-SIGN but not Langerhans cells nor macrophages. Overall, the results suggest that antigen carried by liposomes prepared with Man-tri (**4**) would be more selective *in vivo* for

DCs thanks to better recognition by DC-SIGN. Evaluating the selectivity of the targeting, immune responses and therapeutic efficacy induced upon administration of antigens payloaded liposomes decorated with Tri-Man (**1**) or Man-tri (**4**) would be of great importance. However, a murine model expressing DC-SIGN is imperative. Recently, it was reported that mDC-SIGN mice expressing CD209a/SIGNR5 display overlapping similarities between hDC-SIGN and CD209a/SIGNR5 [38]. A humanized DC-SIGN murine model is also available [39]. These models may be an interesting approach for these investigations after determining whether the binding and uptake of liposomes with Man-tri (**4**) and Tri-Man (**1**) with their DCs are identical to that reported here on hDC.

4. Experimental

All reagents were purchased from Sigma unless otherwise stated and used without further purification. The tri-antenna of α -D-mannopyranoside diether lipid (**Tri-Man**) (**1**) was synthesized as described [40]. 1-azido- β -D-glucopyranoside (**Glc-azide**) (**2a**) and 1-azido- α -D-mannopyranoside (**Man-azide**) (**3a**) were purchased from Sigma.

*4.1. Synthesis of 3,6-di-O-(α -D-mannopyranosyl)- α -D-mannopyranosylazide (Man-tri azide) (**4a**)*

The sugar was synthesized as described [29].

4.2. Synthesis of 5-azidopentanoic acid

The compound was synthesized as described [41, 42]. To a stirred solution of 5-bromovaleric acid (5 g; 27.61 mmol) in dry DMF (50 mL) was added sodium azide (2.15 g; 33.14 mmol;

1.2 eq). The mixture was stirred for 2 h at 80°C, and then diluted with EtOAc (50 mL). The organic phase was washed with brine (2 x 100 mL), water (2 x 100 mL), dried over sodium sulfate, filtered and concentrated. The crude product was purified by “manual” flash chromatography (Cyclohexane/ EtOAc, 5/5) to give the compound (1.90 g; 48%). ¹H NMR (CDCl₃, 300 MHz) δ(ppm) 11.11 (s, 1H, COOH); 3.33 (t, *J* = 6.6 Hz, 2H, CH₂d); 2.43 (t, *J* = 7 Hz, 2H, CH₂a); 1.85-1.55 (m, 4H, CH₂b, CH₂c). ¹³C NMR (CDCl₃, 75 MHz) δppm 179.6 (COOH); 51.0 (C-d); 33.4 (C-a); 28.1(C-c); 21.8 (C-b) (Supplementary Figure 5a).

4.3. Synthesis of 2,4-di-O-benzoyl-3,6-di-O-(2,3,4,6-tetra-O-acetyl-α-D-mannopyranosyl)-β-D-mannopyranosylamido-5-azido-pentanamide

A solution of 2,4-di-O-benzoyl-3,6-di-O-(2,3,4,6-tetra-O-acetyl-α-D-mannopyranosyl)-α-D-mannopyranosylazide [43] (1.5 g, 1.4 mmol) in methanol (30 mL) was hydrogenated in a Hcube (Mode Full H₂, 1 mL.min⁻¹, 25 °C) on a Pd/C 10 % cartridge for 36 h. Methanol was removed under reduced pressure to afford the crude β-amine (1.45 g, 99%) pure enough for the next step. The crude β-amine (1g; 0.95 mmol) was dissolved in dry dichloromethane (CH₂Cl₂) (40 mL) at room temperature and in this addition order 5-azidopentanoic acid (200 mg; 1.15 mmol) beforehand dissolved in dry CH₂Cl₂ (1 mL), HATU (726 mg; 1.91 mmol) and DIPEA (332 μL; 1.94 mmol) were added. The mixture was stirred under argon atmosphere for 36 h, then diluted with CH₂Cl₂ (10 mL), the organic phase washed with saturated NaHCO₃ (2 x 10 mL) and water (2 x 10 mL), dried over sodium sulfate, filtered, and

concentrated. The crude product was purified by “automatic” flash chromatography (H₂O/MeCN, 70/30 to 0/100) to afford the compound (620 mg; 55%). ¹H NMR CDCl₃, 300 MHz) δ(ppm) 8.19-7.40 (m, 10H, 2 C₆H₅COO); 6.52 (d, *J* = 9 Hz, 1H, NHCO); 5.75 (t, *J* = 9.9 Hz, 1H, H-4A); 5.70-5.62 (m, 2H, H-1A + 1H); 5.37 (dd, *J* = 3.4 Hz, *J* = 10Hz, 1H, H-3C); 5.31 (dd, *J* = 1.7 Hz, *J* = 3.4 Hz, 1H, H-2B or H-2C); 5.23 (t, *J* = 10 Hz, 1H, H-4C); 5.09 (t, *J* = 9.6 Hz, 1H, H-4B); 5.00 (dd, *J* = 3.5 Hz, *J* = 9.7 Hz, 1H, H-3B); 4.90 (d, *J* = 1.8 Hz, 1H, H-1B); 4.87-4.81 (m, 2H, H-1C + 1 H); 4.32-3.66 (m, 9H, H-6A, H-6'A, H-6B, H-6'B, H-6C, H-6'C + 3 H); 3.26 (t, *J* = 6.4 Hz, 2H, CH₂d); 2.25 (t, *J* = 6.7 Hz, 2H, CH₂a); 2.11, 2.06, 1.99, 1.97, 1.97, 1.80, 1.77 (7s, 24H, CH₃COO); 1.74-1.55 (m, 4H, CH₂b, CH₂c). ¹³C NMR (75 MHz, CDCl₃) δppm 171.83, 170.64, 170.57, 169.99, 169.73, 169.69, 169.44, 168.84, 166.42, 164.85 (C₆H₅COO, CH₃COO, NHCO); 133.74, 133.59, 130.15, 129.82, 128.8, 128.79, 128.61, 128.50 (C6H₅COO); 99.24, 97.96 (C-1B, C-1C); 76.88 (C-1A); 76.57, 74.72, 71.94, 69.50, 69.46, 69.05, 68.48, 68.08 ([C-2, C-3, C-5]-ABC, C-4A); 66.30 (C-6A); 65.92 (C-4B, C-4C); 62.29 (C-6B, C-6C); 51.03 (C-d); 35.48 (C-a); 28.16 (C-c); 22.23 (C-b); 20.82, 20.67, 20.61, 20.55, 20.36, 20.26 (CH₃COO) (Supplementary Figure 5b). ES-HRMS: [M + Na]⁺ = 1195.3706 m/z calculated for C₅₃H₆₄N₄NaO₂₆; found 1195.3715.

4.4. *Synthesis of 3,6-di-O-(α-D-mannopyranosyl)-β-D-mannopyranosylamido-5-azidopentanamide (Man-tri-spa azide) (5a)*

To a solution of 2,4-di-*O*-benzoyl-3,6-di-*O*-(2,3,4,6-tetra-*O*-acetyl- α -D-mannopyranosyl)- β -D-mannopyranosylamido-5-azido-pentanamide (128.5 mg, 0.122 mmol) dissolved in MeOH (3.5 mL) was added 1M sodium methoxide solution (3.68 mL, 3.68 mmol; 30 equiv.) The mixture was stirred for 7 days at 30°C then neutralized with Amberlite® IR120 H⁺ resin, filtered, and concentrated. The crude product was purified by “automatic” flash chromatography (H₂O/MeCN, 95/5 to 0/100) to afford the compound **5a** (47.7 mg, 69% containing 9% of α anomer). ¹H NMR (D₂O, 300 MHz) δ (ppm) 5.21 (d, *J* = 1 Hz, 1 H, H-1A) 5.11 and 4.84 (2d, *J* = 1.7Hz, 2H, H-1B, H-1C); 4.11-3.55 (m, 18H, H-2A to C, H-3A to C, H-4A to C, H-5A to C, 2 H-6A to C); 3.31 (t, *J* = 6.6 Hz, 2H, CH₂d); 2.34 (t, *J* = 7 Hz, 2H, CH₂a); 1.73-1.48 (m, 4H, CH₂b, CH₂c). ¹³C NMR (75 MHz, D₂O) δ ppm 176.91 (NHCO); 102.13, 99.52 (C-1B, C-1C); 80.69, 77.78, 75.77, 73.41, 72.70, 70.57, 70.38, 70.04, 69.88, 69.80, 66.84, 66.73, 66.66, 65.43 (C-1A, [C-2, C-3, C-4, C-5]-ABC, C-6A); 61.06, 60.96 (C-6B, C-6C); 50.75 (C-d); 34.92 (C-a); 27.43 (C-c); 22.29 (C-b) (Supplementary Figure 5c). ES-HRMS: [M + Na]⁺ = 651.2337 m/z calculated for C₂₃H₄₀N₄NaO₁₆; found 651.2338.

4.5. Synthesis of 2-Aminoethyl 3-*O*-[1-(2-*O*-(α -D-mannopyranosyl)- α -D-mannopyranosyl)-1,2,3-triazol-4-yl]methyl- α -D-mannopyranoside-5-azido-pentanamide (*PMan*₄azide) (**6a**)

A solution of 2-Aminoethyl 3-*O*-[1-(2-*O*-(α -D-mannopyranosyl)- α -D-mannopyranosyl)-1,2,3-triazol-4-yl]methyl- α -D-mannopyranoside hydroformate [29] (84 mg, 0.124 mmol) and DIPEA (22 μ L, 0.129 mmol) in DMF (5 mL) was stirred for 2h at room temperature under

argon. A solution of 5-azidopentanoic acid (18 mg, 0.125 mmol), DIC (40 μ L, 0.253 mmol) and HOBt (34 mg, 0.251 mmol) in DMF (5 mL) was prepared 2 h before use. The two solutions were mixed and stirred for 24 h at 60 °C. DMF was removed *in vacuo*, the crude product passed through a sephadex column and then purified by HPLC to afford compound **6a** (22 mg, 23%) as a white solid. ^1H NMR (D_2O , 400 MHz) δ (ppm) 8.12 (s, 1H, H-5 triazole); 6.28 (d, $J = 1.8$ Hz, H, H-1B); 5.06 (d, $J = 1.3$ Hz, 1H, H-1C); 4.80-4.63 (m, 4H, H-1A, H-2B, $\text{OCH}_2\text{CCHN}_3$); 4.15 (dd, $J = 2.5$ Hz, $J = 6.7$ Hz, 1H, H-3B); 4.07-3.99 (m, 2H, H-2A, H-2C); 3.81-3.25(m, 18H, H-3A, H-3C, H-4A to C, H-5A to C, 2 H-6A to C, CH_2 7, CH_2 8); 3.24 (t, $J = 4.8$ Hz, 2H, CH_2 d); 2.20 (t, $J = 5.55$ Hz, 2H, CH_2 a); 1.62-1.45 (m, 4H, CH_2 b, CH_2 c). ^{13}C NMR (D_2O , 100 MHz) δ ppm 176.59 (NHCO); 144.49 (C-4 triazole); 124.71 (C-5 triazole); 101.96 (C-1C); 99.50 (C-1A); 84.89 (C-1B); 78.66, 76.58, 76.17, 73.49, 72.71, 70.21, 69.83, 69.78, 66.61, 65.84, 65.48, 61.57, 60.91, 60.76, 60.35 ([C-2, C-3, C-4, C-5, C-6]-ABC, C-8 and $\text{OCH}_2(\text{CCHN}_3)$); 50,65 (C-d); 38,80 (C-7); 35.20 (C-c); 27.42 (C-b); 22.69 (C-a) (Supplementary Figure 5d). ES-MS: $[\text{M} + \text{Na}]^+ = 776.3$ m/z calculated for $\text{C}_{28}\text{H}_{47}\text{N}_7\text{NaO}_{17}$; found 776.6.

4.6. Synthesis of 2-Aminoethyl 3,6-di-O-[1-(α -D-mannopyranosyl)-1,2,3-triazol-4-yl]methyl- α -D-mannopyranoside-5-azido-pentanamide (*PMan*₅ azide) (**7a**)

A solution of 2-Aminoethyl 3,6-di-O-[1-(α -D-mannopyranosyl)-1,2,3-triazol-4-yl]methyl- α -D-mannopyranosidehydroformate [29] (150 mg, 0.211 mmol) and DIPEA (36 μ L, 0.211

mmol) in DMF (5 mL) was stirred for 45 min at room temperature under argon. A solution of 5-azidopentanoic acid (31 mg, 0.216 mmol), DIC (71 μ L, 0.455 mmol) and HOBt (54 mg, 0.399 mmol) in DMF (5 mL) was prepared 30 min before use. The two solutions were mixed and stirred for 24 h at 60 °C. DMF was removed *in vacuo*, the crude product passed through a sephadex column and then purified by HPLC to afford compound **7a** (25 mg, 11%) as a white solid. ^1H NMR (D_2O , 400 MHz) δ (ppm) 8.12, 8.11 (2s, 2H, H-5 triazole); 6.03, 6.02 (2d, J = 1.8 Hz, H-1B, H-1C); 4.77-4.60 (m, 7H, H-1A, H-2B, H-2C, 2 x $\text{OCH}_2(\text{CCHN}_3)$); 4.06-4.01 (m, 3H, H-2A, H-3B, H-3C); 3.76-3.58 (m, 13H, H-3A, H-4A to C, H-5A, 2 H-6A to C, CH_2 8); 3.51-3.15 (H-5B, H5-C, CH_2 7, CH_2 d); 2.16 (t, J = 5.4 Hz, 2H, CH_2 a); 1.60-1.40 (m, 4H, CH_2 b, CH_2 c). ^{13}C NMR (D_2O , 100 MHz) δ ppm 176.66 (NHCO); 144.63 and 144.31 (C-4 triazole); 124.92 and 124.89 (C-5 triazole); 99.80 (C-1A); 86.88 (C-1B and C-1C); 78.72, 76.26, 71.60, 70.63, 69.19, 68.42, 68.40, 66.80, 66.65, 66.37, 66.17, 65.67, 63.48, 61.80, 60.59 ([C-2, C-3, C-4, C-5, C-6]-ABC, C-8 and $\text{OCH}_2(\text{CCHN}_3)$); 50.83 (C-d); 39.03 (C-7); 35.39 (C-c); 27.63 (C-b); 22.90 (C-a) (Supplementary Figure 5e). ES-MS: $[\text{M} + \text{Na}]^+ = 857.3$ m/z calculated for $\text{C}_{31}\text{H}_{50}\text{N}_{10}\text{NaO}_{17}$; found 857.5.

4.7. Synthesis of Propargyl-PEG₈-amine

Azide-PEG₈-alcohol (138 mg, 0.35 mmol) (Broadpharm) was solved in 5 ml DMF and cooled to 0°C. NaH (17 mg, 0.7 mmol) was added portion wise and stirred for 10 min at 0 °C before adding of 80% propargyl bromide solution (75 μ l, 0.7 mmol). After stirring overnight at room

temperature, 20 ml water was added and the product was extracted with 2 x 25 ml ether. The organic layer was dried on MgSO₄, filtered and concentrated under pressure. The crude product was purified by silica gel chromatography (CH₂Cl₂/CH₃OH, 95:5) to yield azide product as colorless oil (140 mg, 92%). The azide group was then reduced in amino group in THF/water (4:1; v:v) in the presence of triphenylphosphine (109 mg, 0.45 mmol) under N₂ atmosphere. The alkyne-PEG₈-amine was used in next step without further purification.

4.8. Synthesis of Propargyl-PEG₈-diether

The acid diether lipid (76 mg, 0.124 mmol) prepared as described [40] in 20 ml CH₂Cl₂ containing HBTU (52 mg, 0.136 mmol) was stirred at room temperature for 30 min. Then, the propargyl-PEG₈-Amine (46 mg, 0.113 mmol) and DIPEA (18 mg, 0.136 mmol) were added to the above solution and stirred overnight at room temperature. The solution was washed with aqueous solution of 1N HCl and brine. The organic phase was dried on MgSO₄ and concentrated under reduced pressure. The crude product purified by flash chromatography on silica gel (CH₂Cl₂/CH₃OH, 98/2) yielded alkyned-lipid as colorless oil (92 mg, 80%); R_f = 0.23 (DCM/CH₃OH, 95/5). ¹H NMR (CDCl₃, 600 MHz) δ(ppm) 7.11-7.13 (m, 1H, NH); 4.08 (s, 2H, CH₂C≡CH); 3.89-3.92 (m, 1H, CHC=O); 3.75-3.79 (m, 1H, CH₂-O); 3.54-3.72 (m, 33H, CH₂-O); 3.42-3.50 (m, 4H, CH₂-NH,CH₂-O); 3.32 (s, 1H, CH≡C); 1.06-1.81 (m, 52H, 24CH₂, 4 CH); 0.84-0.87 (m, 18H, 6 CH₃).

4.9. Synthesis of Glycosylated diether Lipids 2-7

Propargyl-PEG₈-diether (10 mg, 0.01 mmol) in 1 ml THF was added into 1 ml water containing glycosyl-azide (0.012 mmol), CuSO₄ (6 mM) and sodium ascorbate (6 mM). The mixture was stirred overnight at room temperature. The glycolipids were purified by silica gel chromatography (CH₂Cl₂/CH₃OH/H₂O, 90/10/1). Yield all >95%. Mass spectra : **Glc (2)** : found 1227.71; theoretical 1227.89. **Man (3)** : found 1227.75; theoretical 1227.89. **Man-tri (4)** : found 1552.11; theoretical 1051.99. **Man-tri-spa (5)** : found 1651.18; theoretical 1651.06. **PMan₄ (6)** : found 1776.36; theoretical 1776.12. **PMan₅ (7)** : found 1857.17; theoretical 1857.16 (Supplementary Figures 6).

4.10. Liposomes

Liposomes **1b-7b** were prepared at 5.4 mM in RNase-free 10 mM Hepes buffer, pH 7.4 (Hepes). Lipids in ethanol were combined in a round bottom flask in a DPPC/DOPE/glycodiether-lipid (**1-7**)/Flu-DOPE ratio of 47.25%:47.25%:5%:0.5%. After removal of the solvent by a rotary vacuum pump, the lipid film was dried for another 30 min in vacuum, and then hydrated with Hepes. The liposomes were then subjected to five cycles of freeze-thaw between Liquid N₂ and 45 °C water bath for 2 min in each step. The size of the liposomes was reduced by extruding 15 times at a mini extruder (Avanti Polar Lipid) through polycarbonate membranes with a final pore size of 200 nm (Nuclepore).

4.11. Size and ζ potential measurements

The size and ζ potential of liposomes were measured in Hepes by using the SZ-100 Analyser (Horiba Scientific).

4.12. Man-Liposomes recognition by lectins

ConA from *Canavalia ensiformis* (Jack bean) binds to terminal α -D-mannosyl and α -D-glucosyl residues with a K_d of $8.75 \cdot 10^{-4}$ M for Me α Man. BC2LA a lectin from *Burkholderia cepacia* displays mannose specificity with a K_d for Me α Man of $2.75 \cdot 10^{-6}$ M [44, 45]. It binds also to all α Man-terminating oligosaccharides. Interactions between liposomes and lectins were measured by GLYcoPROFILE[®] technology from GLYcoDiag (Orléans, France). This method is a lectin array-based assay which uses customized lectin immobilized 96-well plate (LEctPROFILEpalte) (GLYcoDiag) [46]. Samples of liposomes (2.7 mM) were diluted in PBS supplemented with 1mM CaCl₂ and 0.5 mM MgCl₂ and incubated (50 μ L / well) in lectin plates during 1h. After washing with PBS (three times), fluorescence was read with the Fluostar (BMG labtech).

4.13. Cells and cell culture

All reagents were purchased from ThermoFisher Scientific unless otherwise stated and used without further purification. The DC2.4 cell line was a murine dendritic cell line maintained in RPMI supplemented with 10% fetal calf serum (FCS), glutamine (2 mM), penicillin (100 U/mL) and streptomycin (100 μ g/mL) (complete medium) [47]. The DC-SIGN HEK293 cell line – kindly given by O. Schwartz (Pasteur Institute, Paris, France) - was a human cell line

obtained by transduction of HEK293T cells with lentivirus encoding the DC-SIGN human lectin (CD209) [30]. DC-SIGN HEK293 cells grew in DMEM complete medium. All cells grew in humidified air with 5% CO₂ at 37 °C and were Mycoplasma free when checked by using the MycoAlert1 Mycoplasma Detection Kit (Lonza). hMo-DCs were obtained as described [48]. PBMC were freshly isolated from leukapheresis residues (EFS, Paris, France) collected from healthy volunteers after informed written consent). CD14-positive cells were isolated from PBMCs using a magnetic cell sorting (MiltenyiBiotec) and then cultured in the presence of 10% human AB serum RPMI medium, GM-CSF (100 ng/mL; Gentaur) and IL-4 (10 ng/mL; MiltenyiBiotec).

4.14. Binding and uptake of liposomes

Two days before experiments, DC2.4 and DC-SIGN expressing HEK293 cells were seeded in 24-well culture plates (1×10^5 cells/cm²). hMo-DCs were used after for 5 days of culture in the presence of 10% human AB serum RPMI medium, GM-CSF and IL-4. The day of the experiments, the medium was removed, the cells washed with PBS and incubated for 3h with Flu-Lip in serum free medium. Cells were harvested without trypsin, collected into FACS tubes and washed with PBS. The cell-associated fluorescence intensity was measured with a flow cytometer (FORTESSA x 20, Becton Dickinson) with $\lambda_{ex} = 488$ nm; $\lambda_{em} = 530 \pm 30$ nm. The fluorescence intensity was expressed as the mean fluorescence intensity (MFI) of 10 000 cells. Each tube was analyzed three times. The first time in PBS (total fluorescence), the

second time in the presence of Trypan blue (TB) added into the tube at a final concentration of 0.004 % to quench the fluorescein fluorescence associated on the surface of cells. The third time, the fluorescence intensity was measured in PBS in the presence of monensin added 30 min before measurement at a final concentration of 0.03 mg/mL in order to measure the fluorescence intensity upon neutralization of acid intracellular compartments [26, 49].

Acknowledgements

We warmly thank Dr. L. Landemarre from GLYcoDiag (Orléans, France). We thank D. Gosset¹, the P@CYFIC platform at CBM and C. Baillou³ for their technical assistance in flow cytometry. The authors acknowledge Drs. D. Lesur (UMR 7378) and S. Pilard (Plateforme Analytique, UPJV, France) for MS and HPLC. This work was supported by grants from “Région Centre Val de Loire” (APR IR 2015 VACARME project), European Community (Univax:www.UniVax-FP7.eu). Haifei Gao received 2 years fellowship from “Région Centre Val de Loire” (APR IR 2015 VACARME project). We certify that there is no conflict of interest, no competing interest and no disclosure.

References

- [1] C. Fu, A. Jiang, *Front Immunol*, 9 (2018) 3059.
- [2] C.M. Le Gall, J. Weiden, L.J. Eggermont, C.G. Figdor, *Nat Mater*, 17 (2018) 474-475.

- [3] W.W. van Willigen, M. Bloemendal, W.R. Gerritsen, G. Schreibelt, I.J.M. de Vries, K.F. Bol, *Front Immunol*, 9 (2018) 2265.
- [4] B. Wylie, C. Macri, J.D. Mintern, J. Waithman, *Cancers (Basel)*, 11 (2019).
- [5] K.T. Gause, A.K. Wheatley, J. Cui, Y. Yan, S.J. Kent, F. Caruso, *ACS Nano*, 11 (2017) 54-68.
- [6] B.J. Hos, E. Tondini, S.I. van Kasteren, F. Ossendorp, *Front Immunol*, 9 (2018) 884.
- [7] U. Klausen, S. Holmberg, M.O. Holmstrom, N.G.D. Jorgensen, J.H. Grauslund, I.M. Svane, M.H. Andersen, *Front Immunol*, 9 (2018) 2264.
- [8] C.C. Liu, H. Yang, R. Zhang, J.J. Zhao, D.J. Hao, *Eur J Cancer Care (Engl)*, 26 (2017).
- [9] J. Menez-Jamet, C. Gallou, A. Rougeot, K. Kosmatopoulos, *Ann Transl Med*, 4 (2016) 266.
- [10] U. Sahin, K. Kariko, O. Tureci, *Nat Rev Drug Discov*, 13 (2014) 759-780.
- [11] B. Weide, C. Garbe, H.G. Rammensee, S. Pascolo, *Immunol Lett*, 115 (2008) 33-42.
- [12] Z. Xu, P.M. Moyle, *Bioconjug Chem*, 29 (2018) 572-586.
- [13] S.T. Hollmig, K. Ariizumi, P.D. Cruz, Jr., *Glycobiology*, 19 (2009) 568-575.
- [14] H. Tateno, K. Ohnishi, R. Yabe, N. Hayatsu, T. Sato, M. Takeya, H. Narimatsu, J. Hirabayashi, *J Biol Chem*, 285 (2010) 6390-6400.
- [15] J.B. Torrelles, A.K. Azad, L.S. Schlesinger, *J Immunol*, 177 (2006) 1805-1816.
- [16] C.G. Figdor, Y. van Kooyk, G.J. Adema, *Nat Rev Immunol*, 2 (2002) 77-84.

- [17] P.J. Tacken, I.J. de Vries, R. Torensma, C.G. Figdor, *Nat Rev Immunol*, 7 (2007) 790-802.
- [18] T.B. Geijtenbeek, R. Torensma, S.J. van Vliet, G.C. van Duijnhoven, G.J. Adema, Y. van Kooyk, C.G. Figdor, *Cell*, 100 (2000) 575-585.
- [19] A. Cambi, D.S. Lidke, D.J. Arndt-Jovin, C.G. Figdor, T.M. Jovin, *Nano Lett*, 7 (2007) 970-977.
- [20] A. Engering, T.B. Geijtenbeek, S.J. van Vliet, M. Wijers, E. van Liempt, N. Demaurex, A. Lanzavecchia, J. Fransen, C.G. Figdor, V. Piguet, Y. van Kooyk, *J Immunol*, 168 (2002) 2118-2126.
- [21] A. Engering, S.J. Van Vliet, T.B. Geijtenbeek, Y. Van Kooyk, *Blood*, 100 (2002) 1780-1786.
- [22] T. Zhou, Y. Chen, L. Hao, Y. Zhang, *Cell Mol Immunol*, 3 (2006) 279-283.
- [23] E. van Liempt, C.M. Bank, P. Mehta, J.J. Garcia-Vallejo, Z.S. Kavar, R. Geyer, R.A. Alvarez, R.D. Cummings, Y. Kooyk, I. van Die, *FEBS Lett*, 580 (2006) 6123-6131.
- [24] M.A. Boks, M. Ambrosini, S.C. Bruijns, H. Kalay, L. van Bloois, G. Storm, J.J. Garcia-Vallejo, Y. van Kooyk, *J Control Release*, 216 (2015) 37-46.
- [25] C.M. Fehres, H. Kalay, S.C. Bruijns, S.A. Musaafir, M. Ambrosini, L. van Bloois, S.J. van Vliet, G. Storm, J.J. Garcia-Vallejo, Y. van Kooyk, *J Control Release*, 203 (2015) 67-76.
- [26] M. Monsigny, A.C. Roche, P. Midoux, *Biol Cell*, 51 (1984) 187-196.

- [27] W. Yeeprae, S. Kawakami, F. Yamashita, M. Hashida, *J Control Release*, 114 (2006) 193-201.
- [28] V. Cendret, M. Francois-Heude, A. Mendez-Ardoy, V. Moreau, J.M. Garcia Fernandez, F. Djedaïni-Pilard, *Chem Commun* 48 (2012) 3733-3735.
- [29] M. Francois-Heude, A. Mendez-Ardoy, V. Cendret, P. Lafite, R. Daniellou, C. Ortiz Mellet, J.M. Garcia Fernandez, V. Moreau, F. Djedaïni-Pilard, *Chem Eur J* 21 (2015) 1978-1981.
- [30] A. Le Moignic, V. Malard, T. Benvegno, L. Lemiegre, M. Berchel, P.A. Jaffres, C. Baillou, M. Delost, R. Macedo, J. Rochefort, G. Lescaille, C. Pichon, F.M. Lemoine, P. Midoux, V. Mateo, *J Control Release*, 278 (2018) 110-121.
- [31] M. Brard, C. Laine, G. Rethore, I. Laurent, C. Neveu, L. Lemiegre, T. Benvegno, *J Org Chem*, 72 (2007) 8267-8279.
- [32] G.D. Sprott, A. Yeung, C.J. Dicaire, S.H. Yu, D.M. Whitfield, *Archaea*, 2012 (2012) 513231.
- [33] T. Benvegno, L. Lemiegre, C. Ballet, Y. Portier, D. Plusquellec, in: A. Pilar Rauter, T.K. Lindhorst, Y. Queneau (Eds.), *Royal Society of Chemistry, Cambridge*, , 40 (2014,) pp. 341-377.
- [34] M.E. Taylor, K. Drickamer, *Biochem J*, 274 (Pt 2) (1991) 575-580.
- [35] M.E. Taylor, K. Drickamer, *J Biol Chem*, 268 (1993) 399-404.

- [36] M.E. Taylor, K. Drickamer, *Glycobiology*, 19 (2009) 1155-1162.
- [37] N. Sawettanai, H. Leelayuwapan, N. Karoonuthaisiri, S. Ruchirawat, S. Boonyarattanakalin, *J Org Chem*, 84 (2019) 7606-7617.
- [38] S.T.T. Schetters, L.J.W. Kruijssen, M.H.W. Crommentuijn, H. Kalay, J. Ochando, J.M.M. den Haan, J.J. Garcia-Vallejo, Y. van Kooyk, *Front Immunol*, 9 (2018) 990.
- [39] M. Schaefer, N. Reiling, C. Fessler, J. Stephani, I. Taniuchi, F. Hatam, A.O. Yildirim, H. Fehrenbach, K. Walter, J. Ruland, H. Wagner, S. Ehlers, T. Sparwasser, *J Immunol*, 180 (2008) 6836-6845.
- [40] J. Barbeau, L. Lemiegre, A. Quelen, V. Malard, H. Gao, C. Goncalves, M. Berchel, P.A. Jaffres, C. Pichon, P. Midoux, T. Benvegna, *Carbohydr Res*, 435 (2016) 142-148.
- [41] W. Guerrant, V. Patil, J.C. Canzoneri, L.P. Yao, R. Hood, A.K. Oyelere, *Bioorg Med Chem Lett*, 23 (2013) 3283-3287.
- [42] A.J. Perez, H.B. Bode, *J Lipid Res*, 55 (2014) 1897-1901.
- [43] D. Yockot, V. Moreau, G. Demailly, F. Djedaini-Pilard, *Org Biomol Chem*, 1 (2003) 1810-1818.
- [44] E. Lameignere, L. Malinowska, M. Slavikova, E. Duchaud, E.P. Mitchell, A. Varrot, O. Sedo, A. Imberty, M. Wimmerova, *Biochem J*, 411 (2008) 307-318.
- [45] E. Lameignere, T.C. Shiao, R. Roy, M. Wimmerova, F. Dubreuil, A. Varrot, A. Imberty, *Glycobiology*, 20 (2010) 87-98.

- [46] C. Cheneau, F. Coulon, V. Porkolab, F. Fieschi, S. Laurant, D. Razanajaona-Doll, J.J. Pin, E.M. Borst, M. Messerle, C. Bressollette-Bodin, F. Halary, *J Infect Dis*, 218 (2018) 490-503.
- [47] Z. Shen, G. Reznikoff, G. Dranoff, K.L. Rock, *J Immunol*, 158 (1997) 2723-2730.
- [48] F.P. Dupuy, E. Mouly, M. Mesel-Lemoine, C. Morel, J. Abriol, M. Cherai, C. Baillou, D. Negre, F.L. Cosset, D. Klatzmann, F.M. Lemoine, *J Gene Med*, 7 (2005) 1158-1171.
- [49] P. Midoux, A.C. Roche, M. Monsigny, *Cytometry*, 8 (1987) 327-334.

Figure Legends

Figure 1: (A) Structure of the trimannosylated diether lipid (Tri-Man) (**1**). (B) **Glycal azide structures.** 1-azido- β -D-glucopyranoside (**Glc-azide**) (**2a**); 1-azido- α -D-mannopyranoside (**Man-azide**) (**3a**); 1-azido-3,6-di-O-(α -D-mannopyranosyl)- α -D-mannopyranoside (**Man-tri-azide**) (**4a**); 1-N-butylazide, 3,6-di-O-(α -D-mannopyranosyl)- β -D-mannopyranoside (**Man-tri-spa-azide**) (**5a**); 1-ethyl-amino-butylazide Pseudo-Man₄ (**PMan₄-azide**) (**6a**); 1-ethyl-amino-butylazide Pseudo-Man₅ (**PMan₅-azide**) (**7a**).

Figure 2: Synthesis of the Propargyl-PEG₈-diether and glycal-diether lipids

Figure 3: Binding of Mannosylated Liposomes to mannose specific lectins. Flu-liposomes were incubated with (A) ConA or (B) BC2LA lectins linked on plastic. After washing the fluorescence intensity was measured at 520 nm upon excitation at 495 nm. Liposomes (○) Tri-

Man (**1b**); (◆) Glc (**2b**); (□) Man (**3b**); (■) Man-tri (**4b**); (●) Man-tri-spa (**5b**); (▲) PMan₄ (**6b**); (Δ) PMan₅ (**7b**).

Figure 4: Binding and uptake of mannosylated liposomes by DC2.4 cells and DC-SIGN

HEK293 cells. The fluorescence intensity of cells incubated with Flu-liposomes was

measured by flow cytometry and analysis as described in Supplementary Figure 4. Binding of

liposomes on DC2.4 (**Aa**) and DC-SIGN HEK293 (**Ab**) cells. Intracellular quantity of

liposomes in (**Ba**) DC2.4 and (**Bb**) DC-SIGN HEK293 cells. Monensin enhancement in

DC2.4 (**Ca**) and DC-SIGN HEK293 (**Cb**) cells. Liposomes (○) Tri-Man (**1b**); (◆) Glc (**2b**);

(□) Man (**3b**); (■) Man-tri (**4b**); (●) Man-tri-spa (**5b**); (▲) PMan₄ (**6b**); (Δ) PMan₅ (**7b**). MFI

of each sample was measured three times.

Figure 5: Binding and uptake of mannosylated liposomes by hMo-DCs. The fluorescence

intensity of cells incubated with Flu-liposomes was measured by flow cytometry and analysis

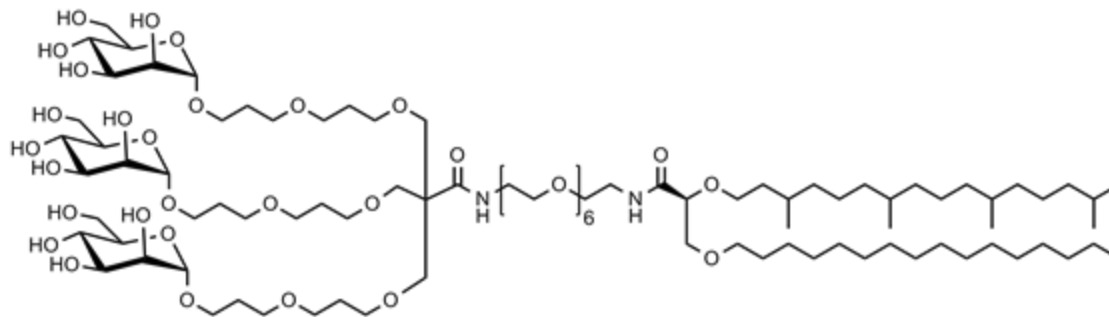
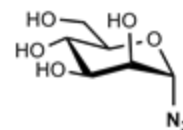
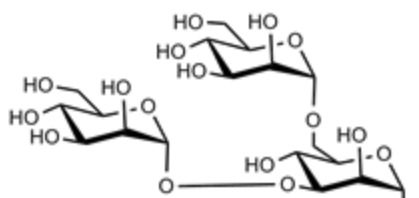
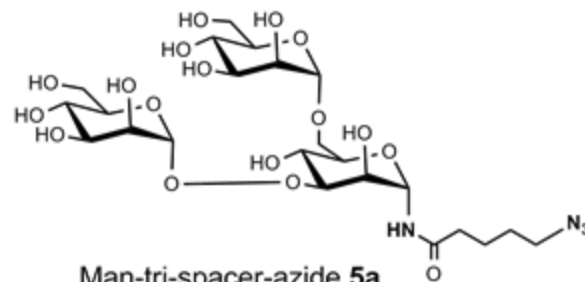
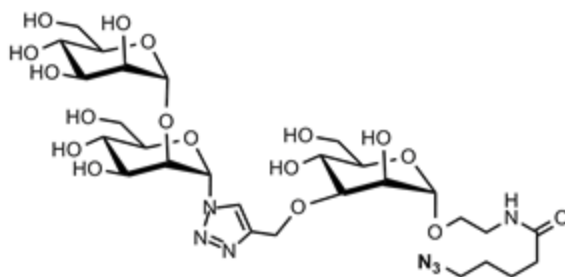
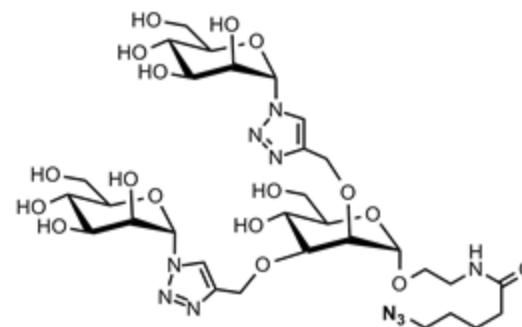
as described in Supplementary Figure 4. (**A**) Binding of liposomes (○) Tri-Man (**1b**); (□) Man

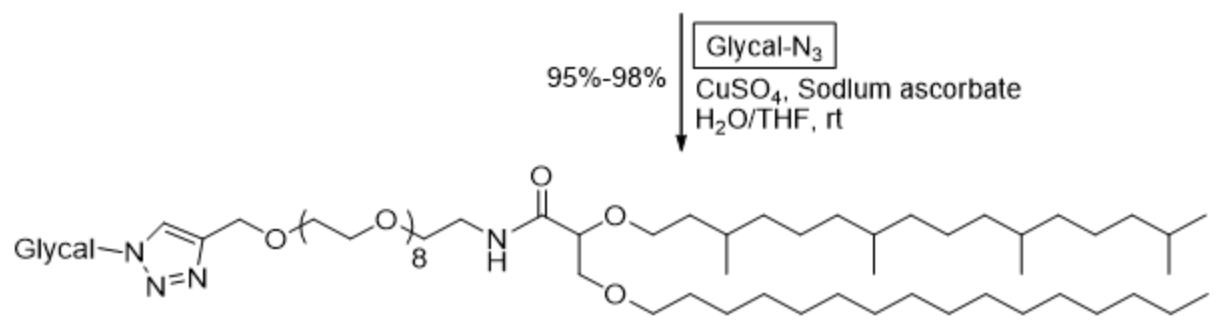
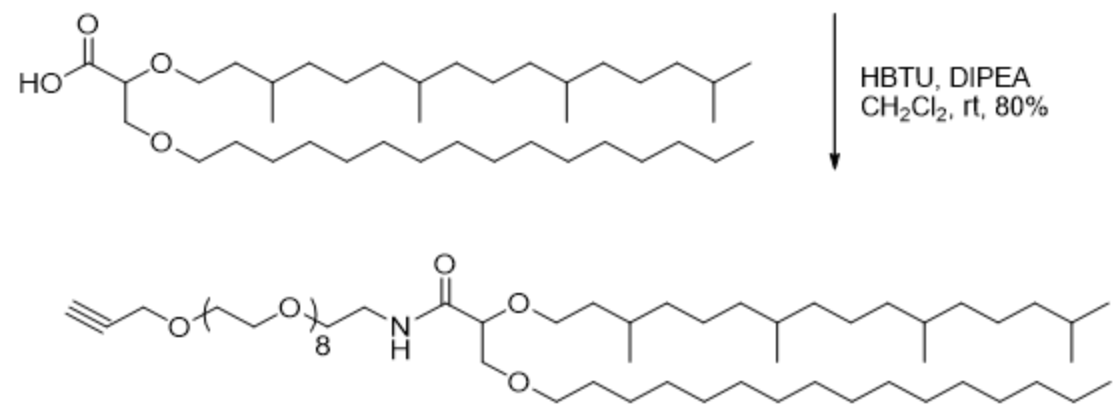
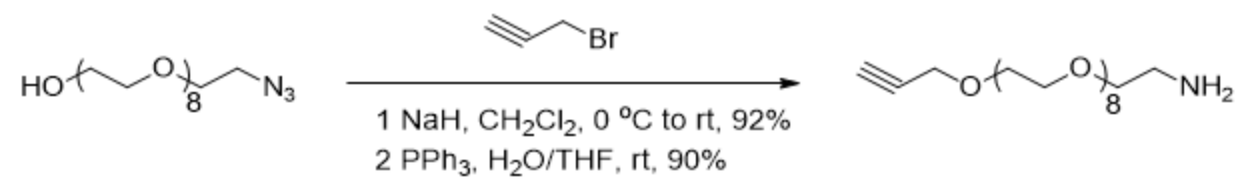
(**3b**); (■) Man-tri (**4b**); (●) Man-tri-spa (**5b**); (▲) PMan₄ (**6b**); (Δ) PMan₅ (**7b**). (**B**)

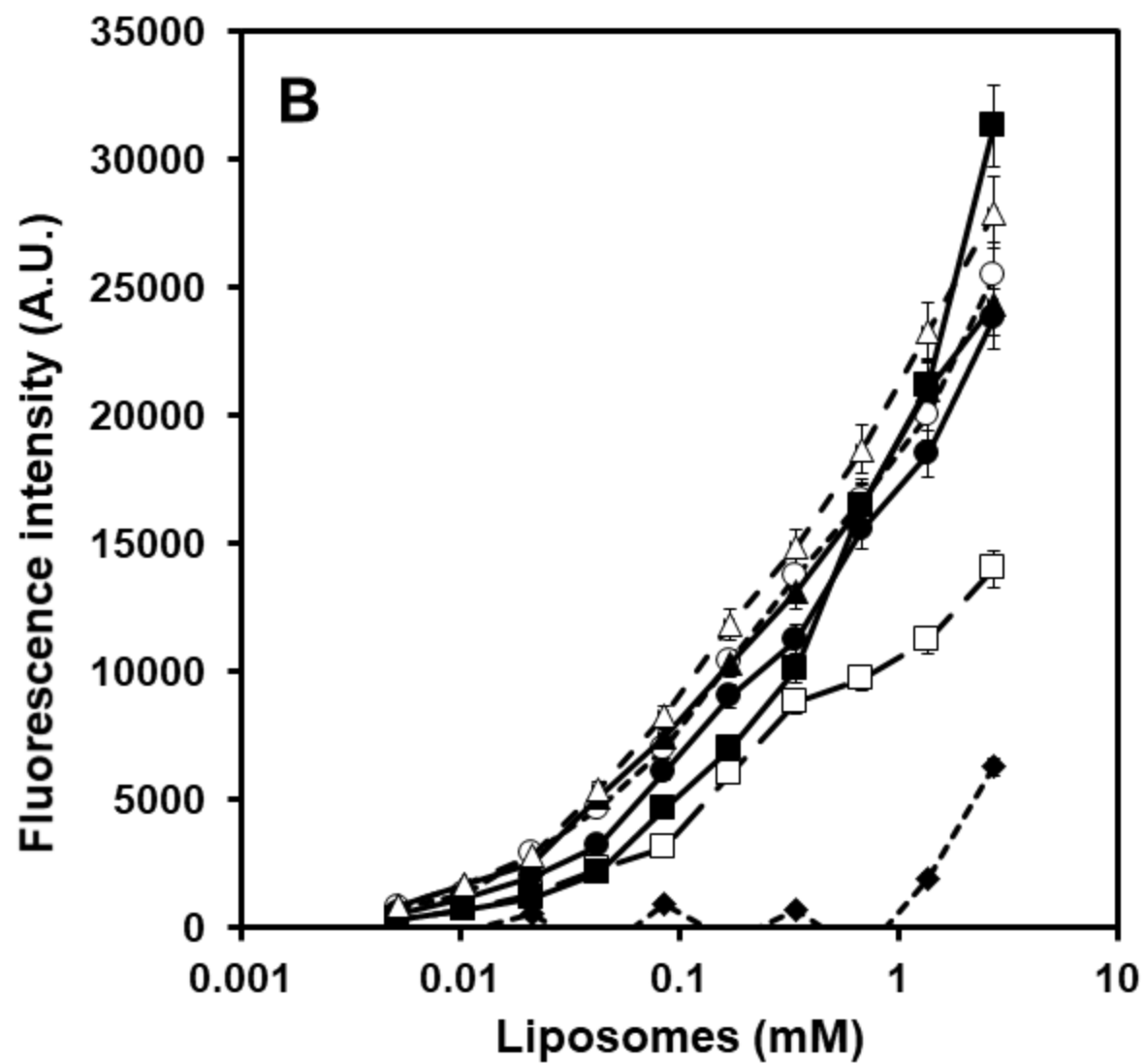
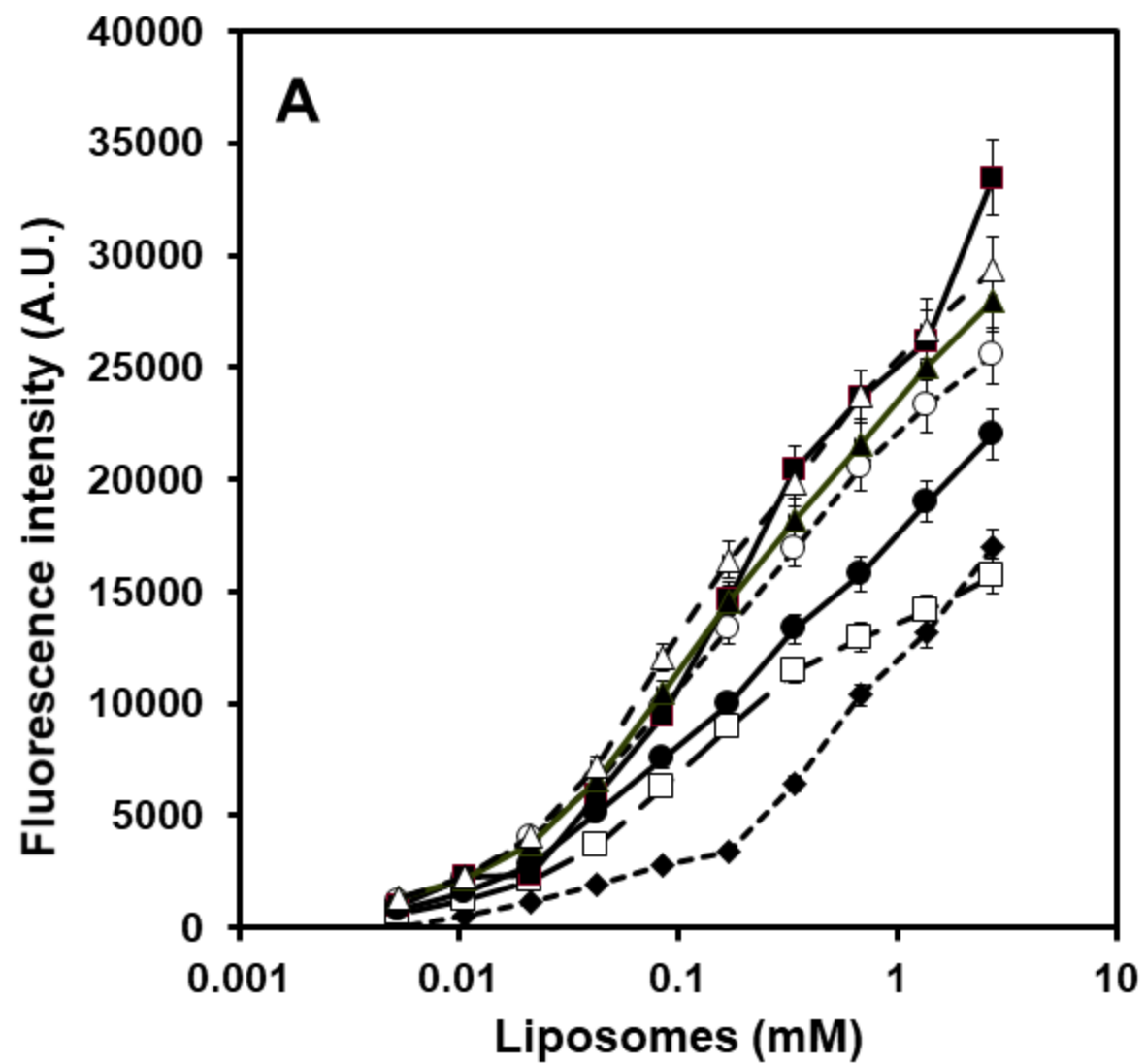
intracellular quantity of liposomes (○) Tri-Man (**1b**); (□) Man (**3b**); (■) Man-tri (**4b**); (●)

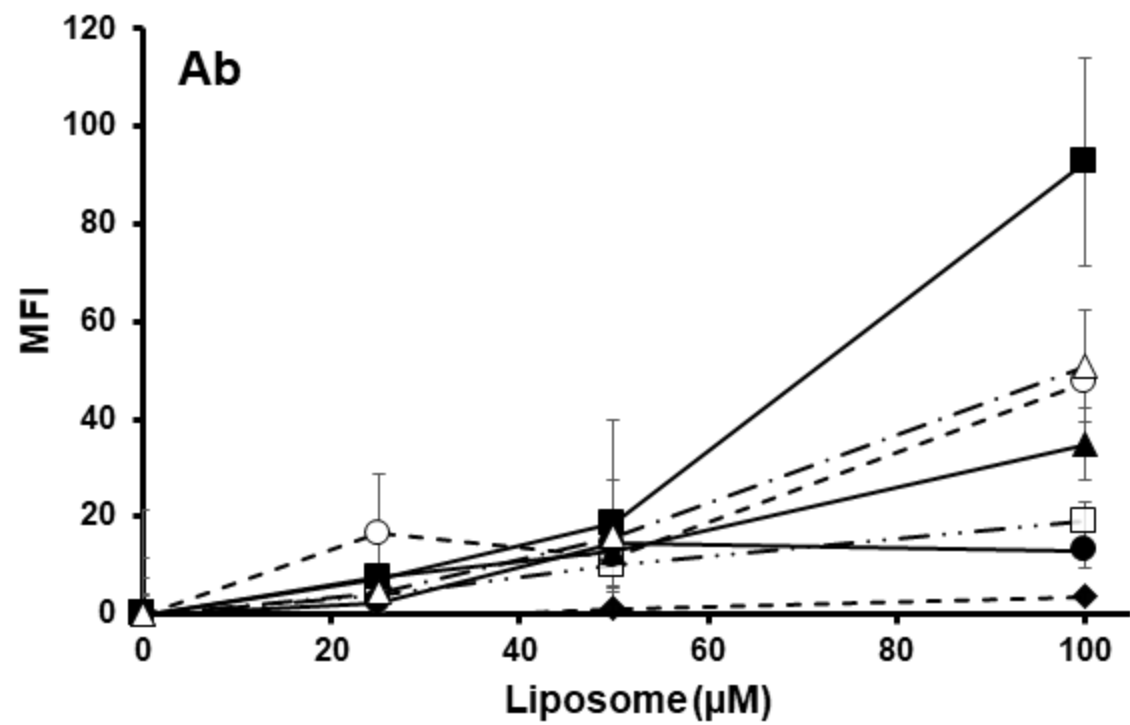
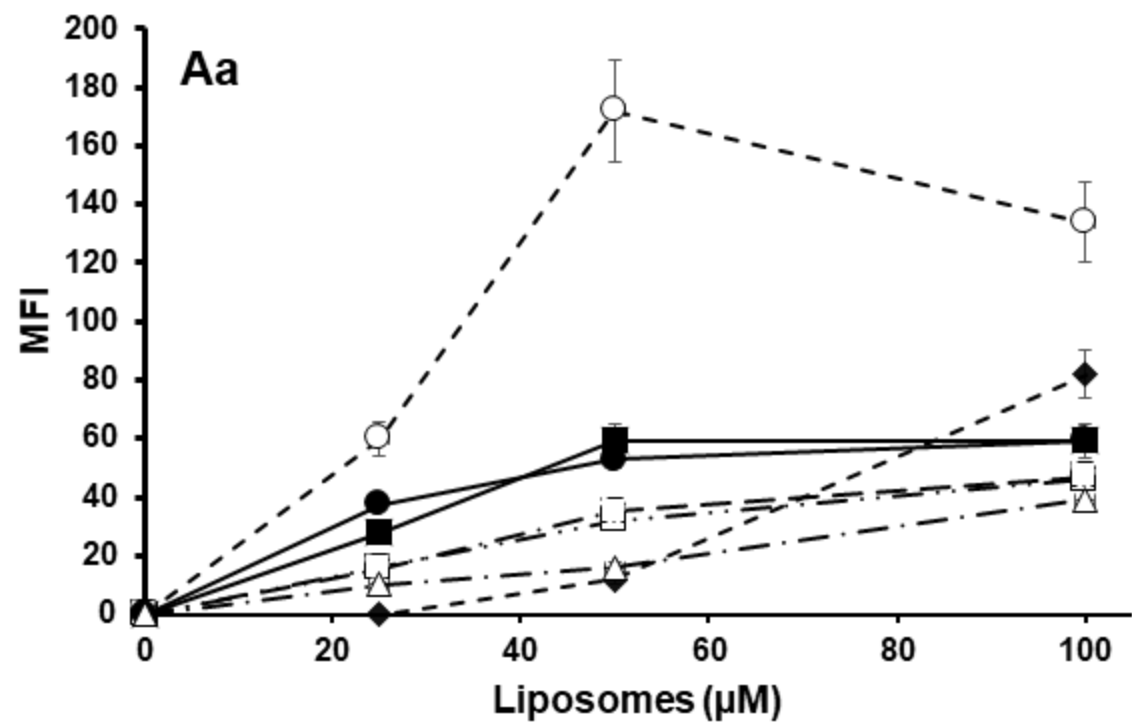
Man-tri-spa (**5b**) or PMan₄ (**6b**) or Glc (**2b**); (Δ) PMan₅ (**7b**). MFI of each sample was

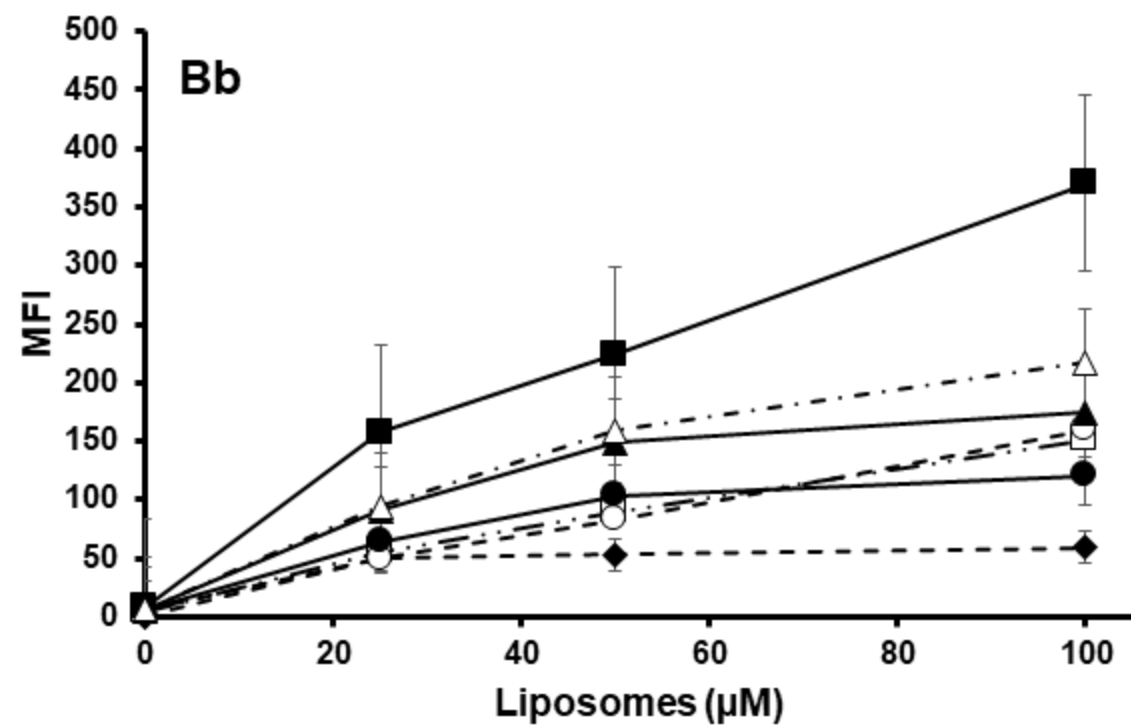
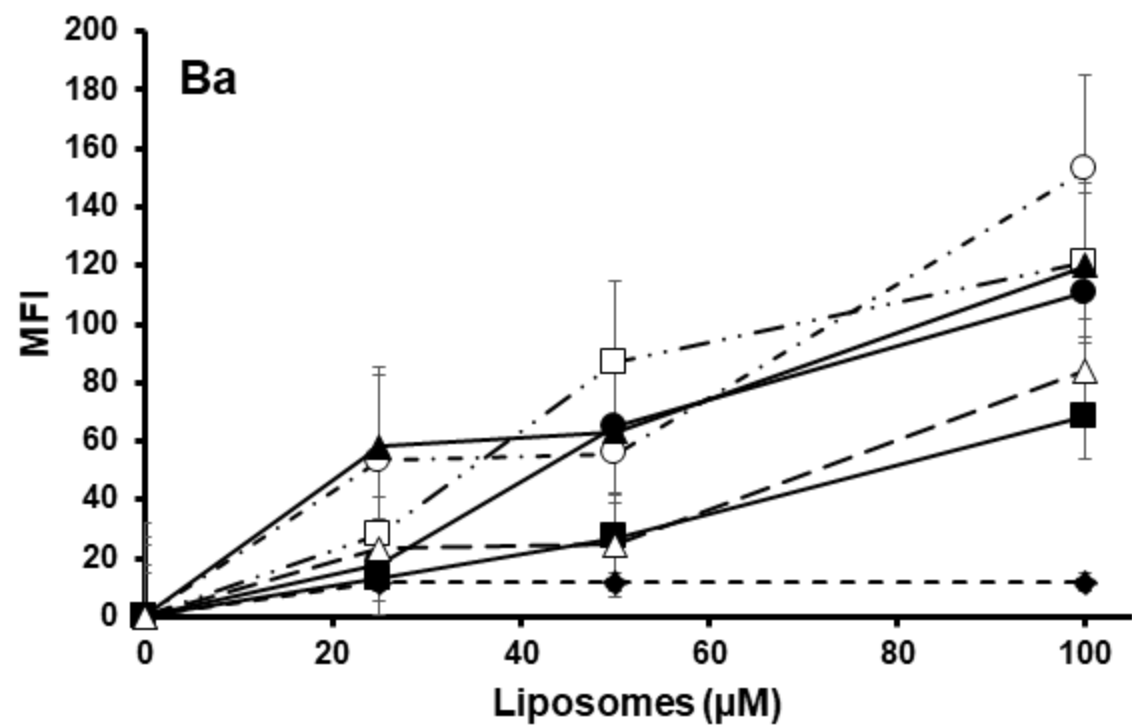
measured three times. MFI of each sample was measured three times.

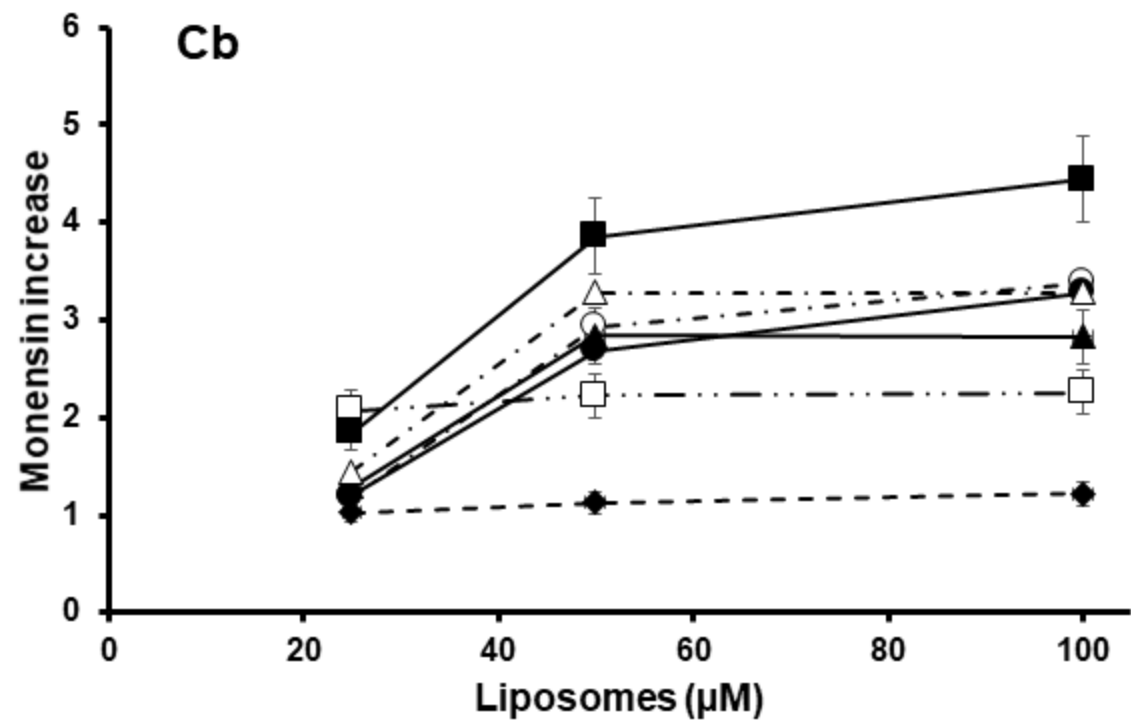
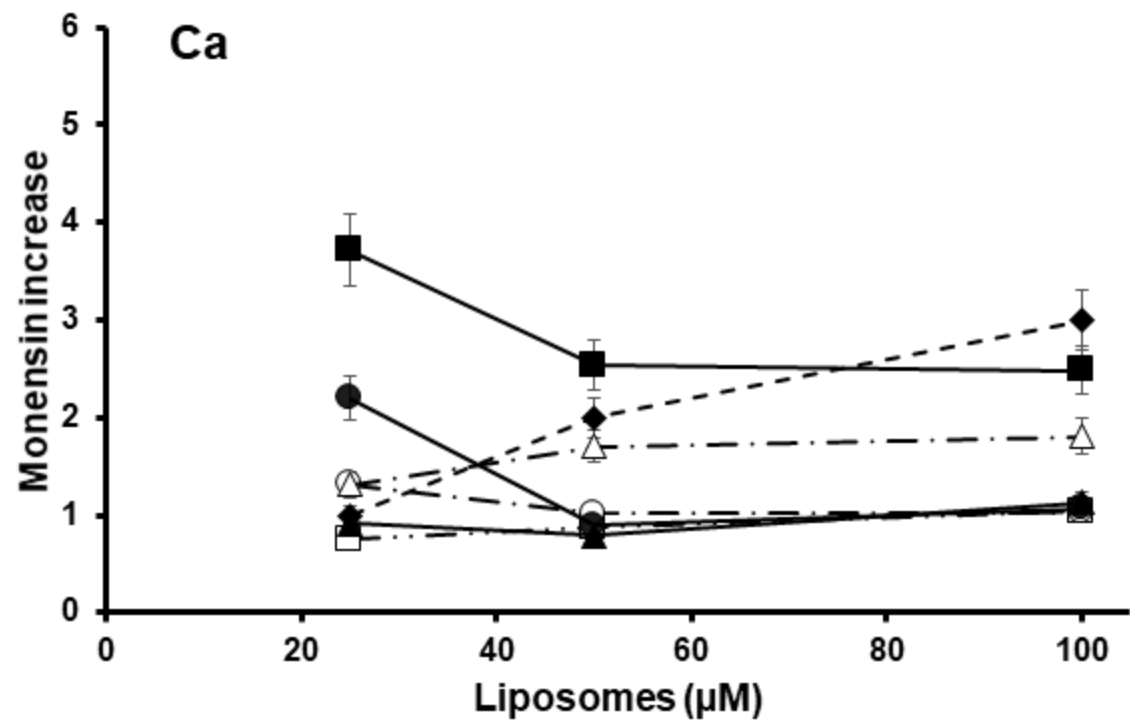
A**Tri-Man-diether 1****B****Glc-azide 2a****Man-azide 3a****Man-tri-azide 4a****Man-tri-spacer-azide 5a****PMan4-azide 6a****PMan5-azide 7a**











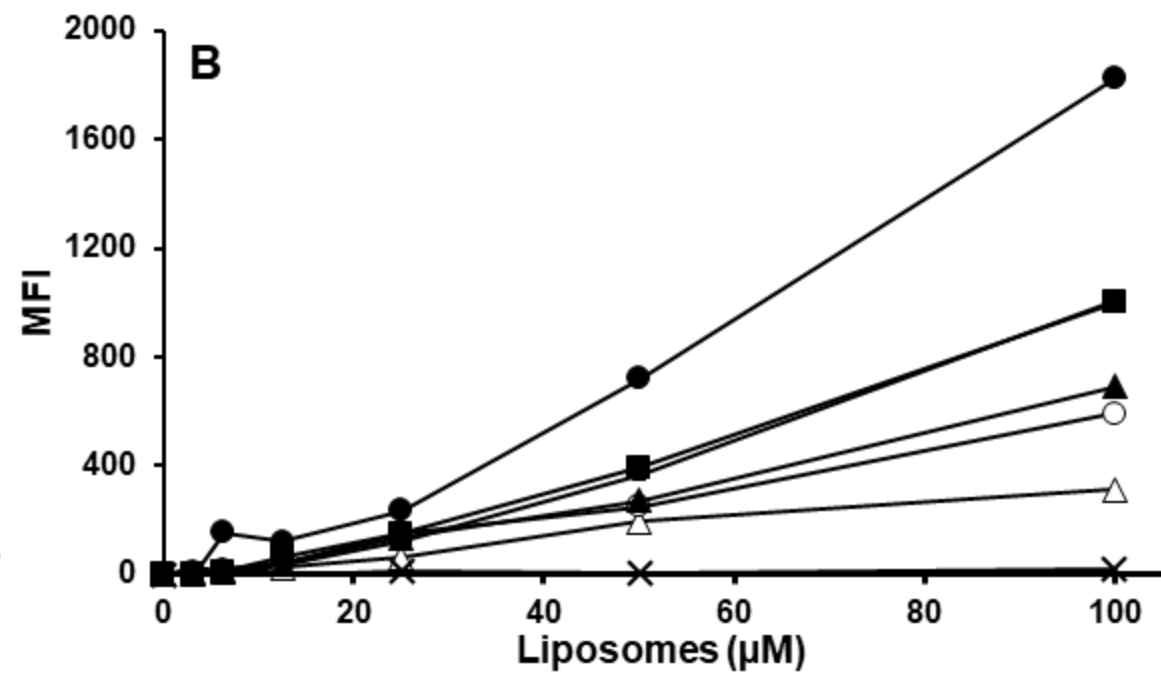
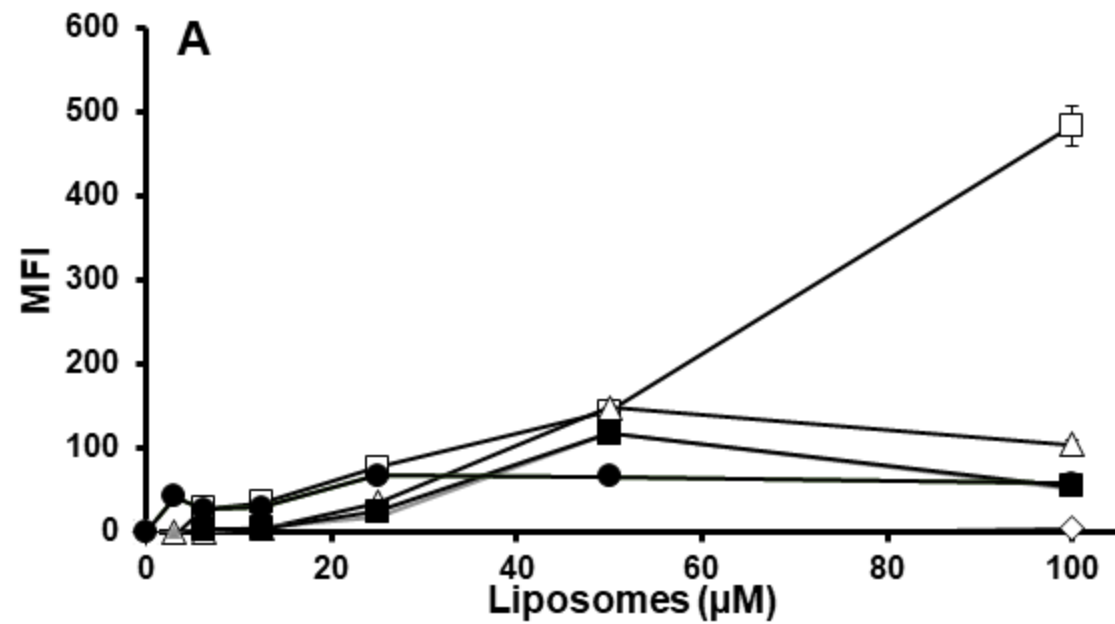


Table I : Size, Polydispersity Index and ζ potential of liposomes

Liposomes	Size (nm \pm S.D.)	PDI	ζ (mv \pm S.E)
No sugar	150 \pm 0.8	0.156	-13 \pm 4
Tri-Man (1b)	154.2 \pm 2.2	0.13	-3.7
Glc (2b)	149.2 \pm 1.7	0.15	-4.5 \pm 0.1
Man (3b)	149.0 \pm 0.7	0.17	-16.0 \pm 1.1
Man-tri (4b)	152.0 \pm 4.1	0.12	-16.0 \pm 0.6
Man-tri-spa (5b)	149.5 \pm 2.0	0.13	-30.0 \pm 2.5
PMan₄ (6b)	155.0 \pm 3.9	0.12	-16.1 \pm 1.1
PMan₅ (7b)	152.6 \pm 1.7	0.14	-33.7 \pm 0.2

